Comparative Medicine
Copyright 2011
by the American Association for Laboratory Animal Science

Vol 61, No 2
April 2011
Pages 109–118

Capacity for Resolution of Ras–MAPK-Initiated Early Pathogenic Myocardial Hypertrophy Modeled in Mice

Bih-Rong Wei,[1] Philip L Martin,[1] Shelley B Hoover,[1] Elizabeth Spehalski,[1,†] Mia Kumar,[1,‡] Mark J Hoenerhoff,[1,#] Julian Rozenberg,[2] Charles Vinson,[2] and R Mark Simpson[1,*]

Activation of Ras signaling in cardiomyocytes has been linked to pathogenic myocardial hypertrophy progression and subsequent heart failure. Whether cardiomyopathy can regress once initiated needs to be established more fully. A 'tet-off' system was used to regulate expression of H-Ras-G12V in myocardium to examine whether Ras-induced pathogenic myocardial hypertrophy could resolve after removal of Ras signaling in vivo. Ras activation at weaning for 2 wk caused hypertrophy, whereas activation for 4 to 8 wk led to cardiomyopathy and heart failure. Discontinuing H-Ras-G12V transgene expression after cardiomyopathy onset led to improved survival and cardiomyopathy lesion scores, with reduced heart:body weight ratios, demonstrating the reversibility of early pathogenic hypertrophy. Activation of Ras and downstream ERK 1/2 was associated with elevated expression of proliferating cell nuclear antigen and cyclins B1 and D1, indicating cell-cycle activation and reentry. Coordinate elevation of broad-spectrum cyclin-dependent kinase inhibitors (p21, p27, and p57) and Tyr15 phosphorylation of cdc2 signified the activation of cell-cycle checkpoints; absence of cell-cycle completion and cardiomyocyte replication were documented by using immunohistochemistry for mitosis and cytokinesis markers. After resolution of cardiomyopathy, cell-cycle activators and inhibitors examined returned to basal levels, a change that we interpreted as exit from the cell cycle. Cardiac cell-cycle regulation plays a role in recovery from pathogenic hypertrophy. The model we present provides a means to further explore the underlying mechanisms governing cell-cycle capacity in cardiomyocytes, as well as progression and regression of pathogenic cardiomyocyte hypertrophy.

Abbreviations: ANF, atrial naturetic factor; ERK1/2, extracellular signal-regulated kinase 1/2; HW:BW, ratio of heart weight to body weight; MAPK, mitogen-activated protein kinase; PCNA, proliferating-cell nuclear antigen.

Persistent cardiac stress can lead to pathogenic myocardial hypertrophy accompanied by arrhythmias, diastolic dysfunction, and ultimately heart failure.[32] A variety of intracellular signaling pathways, including the Ras–mitogen-activated protein kinase (MAPK) pathway, are involved in the development of cardiac hypertrophy.[8,28,31] Ras has been associated with cardiac hypertrophy secondary to pressure overload and other hypertrophic stimuli, including phenylephrine and endothelin 1.[14,25,31,33] Increased Ras expression was correlated with the degree of disease severity in human cardiomyopathy.[13] An active form of Ras (H-Ras-G12V), typically a strong cytoproliferative stimulant in most cell types, has been used experimentally to induce hypertrophic responses in cardiomyocytes. The activation of Ras caused changes that resemble some human myocardial diseases, including increased cell size and reactivation of fetal genes.[35] Production of atrial naturetic factor (ANF), a hallmark of cardiomyocyte hypertrophy, was inhibited by a dominant-negative form of Ras (Ras-15A).[35] Collectively, this evidence demonstrated that Ras activation in cardiomyocytes can result in cardiac hypertrophy.

Transgenic mouse models targeting Ras activation in the heart have been developed.[11,28,41] Ras activation initiated during embryonic development resulted in left ventricular diastolic dysfunction with myofibrillar disarray.[11] Another transgenic model permitting temporal regulation of Ras activation driven by the α-myosin heavy chain promoter resulted in ventricular arrhythmias in 10- to 20-wk-old adult mice.[28] Such models, mimicking features of human myocardial diseases, further establish a role for Ras in pathogenic myocardial hypertrophy.

Although existing *ras* transgenic mouse models provide the opportunity to investigate cardiomyocyte hypertrophy during Ras activation,[20] once induced, Ras stimulation leading to hypertrophy in these models is irreversible. A surgical model has provided a means to reverse pressure overload-induced myocardial hypertrophy by placing a temporary aortic ligature that subsequently is removed.[29] However, this model requires considerable surgical expertise. No system thus far permits controlled stimulation followed by discontinuation by means of genetic manipulation. Such a system would help evaluate whether discontinuing activation of target genes, such as *ras*, in injured hearts results in recovery from hypertrophy.

Ras-induced pathogenic myocardial hypertrophy was investigated in the present study by using a 'tet-off' controlled cardiac

Received: 07 Sep 2010. Revision requested: 14 Oct 2010. Accepted: 03 Nov 2010.
[1]Laboratory of Cancer Biology and Genetics, and [2]Laboratory of Metabolism, Center for Cancer Research, National Cancer Institute, Bethesda, Maryland.
[*]Corresponding author. Email: ms43b@nih.gov
Current affiliation: [†]Department of Molecular and Cellular Pathology, College of Medicine, University of Michigan, Ann Arbor, Michigan; [‡]Laboratory of Human Carcinogenesis, Center for Cancer Research, National Cancer Institute, Bethesda, Maryland; and [#]Molecular and Cellular Pathology Branch, National Institute of Environmental Health Sciences, Research Triangle Park, North Carolina.

H-Ras-G12V transgenic mouse model. In this model, a cardiac-specific α-myosin heavy chain promoter drives expression of the tetracycline transactivator, which in turn initiates expression of active Ras (H-Ras-G12V) in the absence of tetracycline or its analogs. Expression of the Ras-G12V mutant results in a constitutively activated form of Ras protein insensitive to inhibitory GTPase-activating proteins.[23] The model provided opportunities to examine heart tissue for evidence of recovery after discontinuation of Ras activation due to the controllable nature of the transgene expression. In addition to phenotypic changes in heart tissue during the expression and subsequent discontinuation of Ras, the activation status of Ras signaling events and potential for changes in cell-cycle activities were studied.

Materials and Methods

Animals and experimental group design. Mice (*Mus musculus*) with cardiac-specific, doxycycline-controlled H-Ras-G12V (Ras-12V) expression were generated from 2 transgenic lines. The first inbred line (designated M mice, FVB.Cg-Tg(Myh6-tTA)6Smbf/J, http://jaxmice.jax.org/strain/003170.html) carried the tetracycline transactivator gene controlled by rat cardiac α-myosin heavy chain promoter (Jackson Laboratory, Bar Harbor, ME).[40] A second inbred line has an activated human Ras-12V transgene under the control of a minimal promoter containing multimerized tetracycline operons (R mice, FVB-Tg (tetO-HRAS)65Lc, http://mouse.ncifcrf.gov/available_details.asp?ID=01XB4). R mice were obtained from the Repository of Mouse Models of Human Cancers Consortium (NCI-Frederick, Frederick, MD). This mouse was used similarly to our present application to demonstrate reversible expression of Ras in mouse skin.[23] Mice were housed on corncob bedding under a 12:12-h light:dark cycle. Sentinel health surveillance in the colony for the period of the study revealed serologic evidence of murine norovirus only; findings for all other mouse pathogens evaluated (NCI-Frederick) were negative. The current investigation conformed to the *Guide for the Care and Use of Laboratory Animals*[12] and was performed under review by the Institutional Animal Care and Use Committee.

Binary transgenic M/R mice were generated by crossing M and R mice. The expression of Ras-12V was regulated by using dietary doxycycline, included in a mouse ration at 200 mg/kg (Harlan, Frederick, MD). Doxycycline was used to inhibit binding of the tetracycline transactivator protein to tetracycline operons and therefore prevent Ras-12V expression ('Ras off'), whereas regular mouse chow without doxycycline supplementation permitted binding of tetracycline transactivator to tetracycline operons and subsequent transcriptional initiation of Ras-12V expression ('Ras on'). Mice were kept on doxycycline diet at all times except during designated Ras-12V induction periods. Control mice were fed accordingly to avoid potential effects in phenotype caused by doxycycline. During breeding and while nursing, mice were maintained on diet with doxycycline to inhibit Ras-12V expression so that litters of M/R pups could be raised.

The schedule for altering Ras activation is shown in Figure 1 A. Studies were initiated when mice were weaned (3 wk old), at which time M/R mice were divided randomly into 3 cohorts for various cardiac Ras-12V expression durations, for which doxycycline-containing diet was replaced by regular diet for 2, 4, or 8 wk. Mice receiving 2 or 4 wk Ras activation were subdivided into 3 groups each for which dietary doxycycline was reintroduced to discontinue Ras activity, leading to Ras-off periods of 0, 1, or 4 wk. Control mice, including wild-type, M, and R littermates, were treated accordingly. M/R mice maintained continuously on doxycycline (Ras-off) were included as genotype-matched controls. The numbers of animals in each group range from 21 to 53 (Figure 1 A) with a female:male ratio of 1:1.

Mice were monitored for clinical evidence of cardiac disease and indications of hunched posture, scruffy fur, dyspnea, and abdominal distention. At the conclusion of each treatment period, mice were euthanized (carbon dioxide inhalation) and necropsied; body and heart weights were recorded. Subsequently hearts were opened and specimens collected; cardiac tissue from ventricles was preserved either by formalin fixation and paraffin embedding or by embedding in OCT medium (Sakura Finetek, Torrance, CA) and snap-freezing, for later tissue sectioning and other analyses. Selected control and M/R mice underwent complete pathologic examinations including histopathology of all major organs. No evidence of intercurrent background disease was observed. Frozen and formalin-fixed paraffin-embedded tissue sections were stained with hematoxylin and eosin and evaluated histologically. Without knowledge of treatment group, a single pathologist assigned myocardial lesion scores across the entire study by using criteria established for this study (Figure 2) . Each heart was scored 0 to 3 according to affected area, changes in cardiomyocyte morphology, degree of cardiomyocyte degeneration, and quantity of leukocyte infiltration. Fibrosis was taken into consideration by using tissue sections stained with Masson trichrome.

Statistical analysis of lesion score and comparison of ratios of heart weight to body weight (HW:BW) among experimental groups were performed by using the Mann–Whitney test for nonparametric data. Statistical analysis of survival curve data was performed by using a log-rank Mantel–Cox test. Statistical differences were accepted at a P value of 0.05 or less. Analyses were performed using Prism (version 5.03, GraphPad Software, La Jolla, CA).

Immunohistology. Immunohistochemistry was performed as described previously with minor modifications.[38] Briefly, antigen retrieval for paraffin-embedded tissues was performed by immersing tissues in Target Antigen Retrieval Buffer (DakoCytomation, Carpinteria, CA) for 15 min in a steamer (Black and Decker, Hunt Valley, MD). Primary antibodies were followed by biotinylated goat antirabbit IgG secondary antibody (DakoCytomation). Immunoreactions were developed by using a peroxidase-based streptavidin detection method (Vector Labs, Burlingame, CA) and 3,3'-diaminobenzidine tetrahydrochloride (Invitrogen, Carlsbad, CA) as the chromogen substrate. Negative reaction control included substitution of antibody diluent for primary antibodies on tissue sections.

For immunofluorescent assays, antibodies were applied to tissue sections in the following order: antiRas, goat–antirabbit IgG-Dylight 488, antiphospho-extracellular signal-regulated kinase 1/2 (pERK1/2), and goat antirabbit IgG-Dylight 549. Slides were washed with Tris-buffered saline containing 0.02% Tween 20 between antibody incubations. Labeled tissue sections were counterstained and mounted by using mounting medium containing 4',6-diamidino-2-phenylindole (Vectashield Hardset, Vector Labs). Images were captured (Axioskop 2 Plus microscope equipped with AxioCam, Zeiss, Thornwood, NY) by using appropriate filters.

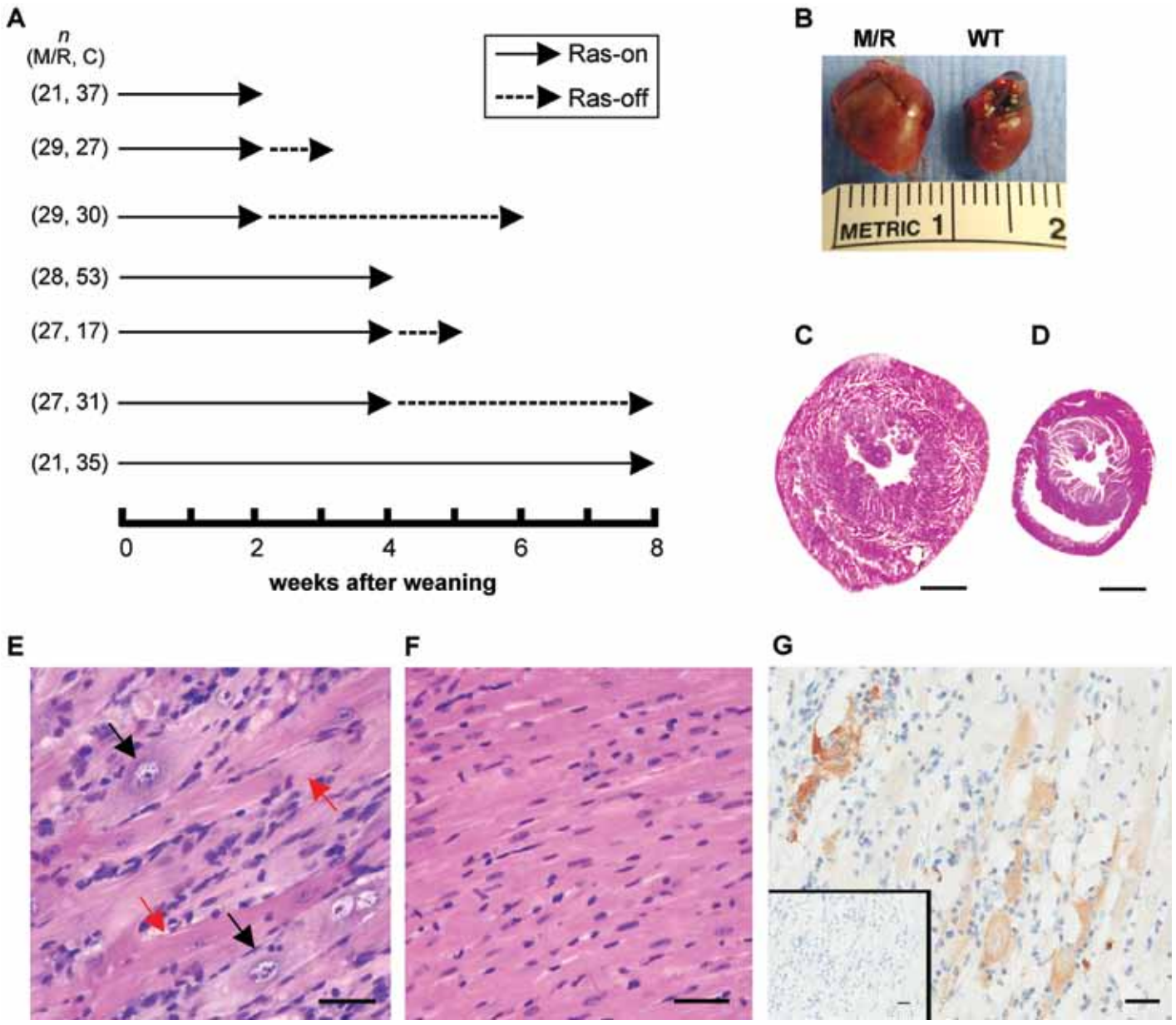

Figure 1. Study design, experimental animal groups, and hypertrophic phenotype induced by Ras activation. (A) Cardiac specific expression of the Ras-12V transgene was activated for different periods of time through use of a tet-off system in M/R mice (Ras-on, solid arrow). Mice experienced 2 wk or 4 wk of Ras activation, after which Ras activation was discontinued for 0, 1, or 4 wk (Ras-off, dashed arrow). A group of mice receiving 8 consecutive weeks of Ras-12V expression served as late-stage disease controls for mice afforded 4 wk of recovery after 4 wk of Ras activation. Additional control mice within each treatment included wild type (WT), M, R, and M/R mice with no Ras-12V transgene expression. Numbers (*n*) of animals in each group (M/R, control [C]) are indicated. (B) Gross photograph of representative hearts from an M/R mouse with heart enlargement (left) and a WT mouse. (C, D) Representative photomicrographs of biventricular short-axis (transverse) tissue sections from (C) an M/R heart (4 wk Ras-on) with pathogenic myocardial hypertrophy and (D) a WT heart. Hematoxylin and eosin stain; bar, 1 mm. (E) Hypertrophic cardiomyocytes with multiple enlarged nuclei (karyomegaly, black arrows) interspersed among less affected cardiomyocytes (red arrows) in a tissue section from a representative M/R mouse heart (4 wk Ras-on). Interstitial cellularity was increased. Hematoxylin and eosin stain; bar, 15 µm. (F) Essentially normal cardiomyocytes from a representative control mouse, shown for comparison. Hematoxylin and eosin stain; bar, 15 µm. (G) Immunohistochemical labeling of active caspase 3 in hypertrophic cardiomyocytes, indicating ongoing apoptosis during advanced-stage cardiomyopathy in M/R mice with 8 wk of Ras activation. Positively labeled myocytes (brown chromogen) are featured by vacuolization and loss of striations. Mononuclear cells infiltrate amid degenerate cardiomyocytes in areas often associated with fibrosis and positive active caspase 3 labeling. Chromogen, 3,3′-diaminobenzidine tetrahydrochloride. (Insert photomicrograph): Serial tissue section of heart shown in G, with antibody preabsorbed with active caspase 3 derived immunogenic peptide, used as control. Chromogen, 3,3′-diaminobenzidine tetrahydrochloride. Bar, 25 µm.

	Lesion score			
	0	1	2	3
(1) Affected myocardial area	0%	≤10%	10% to 40%	>40%
(2) Pathological hypertrophic myocardial phenotype	none	Few changes, dispersed throughout	Moderate to markedly enlarged fibers	Severe
(3) Cardiac myocyte degeneration	none	Few cells, mostly vacuolization	Multifocal involvement	Frequent, coalescing foci
(4) Inflammation and fibrosis	none	Absent or mild*	Limited area, cellular infiltrate, and fibroplasia	Focally intense accumulations

Figure 2. Criteria developed for assigning semiquantitative histopathologic myocardial lesion scores for M/R and control mice include 4 parameters: (1) affected myocardial area: assessment of affected area represented estimates of affected surface area made from examining 5 microscopic fields by using the 10× objective lens, thereby permitting evaluation of the entire cross-sectional area of tissue sections taken from the midregions through both ventricles; (2) pathologic hypertrophic myocardial phenotype: phenotypes included myofiber hypertrophy, anisocytosis, anisokaryosis, and karyomegaly distinguishable from that of control mouse hearts, which may have had occasional enlarged nuclei within normal cardiac myofiber cytomorphology; (3) cardiac myocyte degeneration: signs of cardiac myocyte degeneration included myofiber vacuolization, fragmentation, and loss of cross striations. Other features included occasional necrosis or apoptosis and mineralization of cells; and (4) inflammation and fibrosis: evaluations for inflammation and fibrosis included assessments for mononuclear leukocyte infiltration and interstitial connective tissue. *, Combinations of mild infrequent hypertrophy accompanied by limited inflammation and fibrosis were assigned a lesion score 1 and interpreted to represent some degree of resolution of pathogenic myocardial hypertrophy. These changes were included with more mild hypertrophic changes in the absence of any significant inflammation and fibrosis within lesion score 1, observed during induction.

Antibodies for immuohistochemistry and immunofluorescence included Ras, and Aurora B kinase (Abcam, Cambridge, MA); active (cleaved) caspase 3, pERK1/2, and phospho-histone H3 (Cell Signaling Technology, Danvers, MA); biotin- labeled secondary antibodies were from Dako; Dylight 488-, and Dylight 549-conjugated secondary antibodies were obtained from Jackson ImmunoResearch (West Grove, PA). Cleaved-active caspase 3 blocking peptide was purchased from Cell Signaling Technology.

Western blot analyses. Snap-frozen tissue samples of ventricles were disrupted by placing them in lysis buffer (20 mM Tris-HCl pH 7.5, 150 mM NaCl, 1 mM EDTA, 1 mM EGTA, 1% Triton, 0.1% SDS, 2.5 mM sodium pyrophosphate, 1 mM β-glycerophosphate, 1 mM sodium orthovanadate, and 1 µg/mL leupeptin), vortexing (Biovortexer, Bellco Glass, Vineland, NJ), and incubating at 4 °C for 30 min. Aliquots (10 µg) of clarified tissue protein lysates were separated on 4%-to-20% Tris-glycine gradient gels (Invitrogen Life Technologies) and transferred to polyvinylidene fluoride membranes (Bio-Rad Laboratories, Hercules, CA). The membranes were blocked in 3% bovine serum albumin and incubated with primary antibodies followed by peroxidase-conjugated secondary antibodies. Antibody reactivity was detected by using an electrochemiluminescent Western blot detection reagent (Amersham Biosciences, Piscataway, NJ). Signals from detected proteins were compared qualitatively between specimens from study mice and those in the control groups. Protein expression levels detected in control animals were defined as basal levels. Analyses were performed on individual samples from 9 control and 22 M/R hearts in the 2-wk Ras-on cohort and 11 control and 15 M/R hearts in the 4-wk Ras-on cohort.

Antibodies for the following proteins were used: Ras and cyclin D1 (Abcam); GAPDH, pERK1/2, ERK1/2, cyclin B1, cyclin E, phospho-Cdc2 (Tyr15), c-Jun-NH_2-terminal kinase, phospho-c-Jun-NH_2-terminal kinase, p38, phospho-p38 and proliferating-cell nuclear antigen (PCNA; Cell Signaling Technology); p57 (Epitomics, Burlingame, CA); p21 and cyclin A (Santa Cruz, Santa Cruz, CA); p27 (BD, Franklin Lakes, NJ); and ANF (Peninsula Laboratory, San Carlos, CA); horseradish peroxidase-conjugated secondary antibodies were obtained from Jackson ImmunoResearch.

Results

Pathogenic myocardial hypertrophy in a cardiac Ras transgenic mouse model. Cardiomyopathy and heart enlargement frequently occurred in M/R mice with Ras activation for 4 wk or more (Figure 1 B). The pathogenic myocardial hypertrophy induced by Ras activation progressed to heart failure characterized by systemic vascular congestion, pleural effusion, and ascites in mice with cardiac Ras activation for 4 wk or longer. Ventricular free walls and septae in M/R mice were thickened due to hypertrophy and had grossly reduced ventricular chambers (Figure 1 C), compared with those of control hearts (Figure 1 D). Histologically, hypertrophic cardiomyocytes exhibiting increased cell and nuclear size were interspersed among less-affected myocytes (Figure 1 E). Mononuclear cell infiltration was observed at the disease-affected area (Figure 1 E), in contrast to control hearts (Figure 1 F). Detection of active caspase 3 in hypertrophic cardiomyocytes with 8 wk of Ras activation indicated an association between advanced cardiac disease and cardiomyocyte loss due to programmed cell death (Figure 1 G).

Discontinuation of Ras activity after induction of pathogenic myocardial hypertrophy led to resolution of cardiomyopathy. Cardiac Ras activation for 8 wk resulted in removal of 9 of 21 (43%) M/R mice from the study due to heart failure (Figure 3). By contrast, when the 8-wk study period was divided into 4 wk of Ras activation followed by 4 wk during which Ras activation was discontinued, mortality decreased to 4%, as 26 of 27 (96%) mice escaped the fatal effects of Ras signaling. The significant ($P < 0.001$) difference in survival between the 2 groups indicated that withdrawing Ras signaling after induction of pathogenic hypertrophy provided a survival benefit. Whether improved survival was associated with disease resolution was studied next.

Semiquantitative histopathologic lesion criteria were adopted for assigning cardiac lesion scores to all mice (Figure 2). After 2

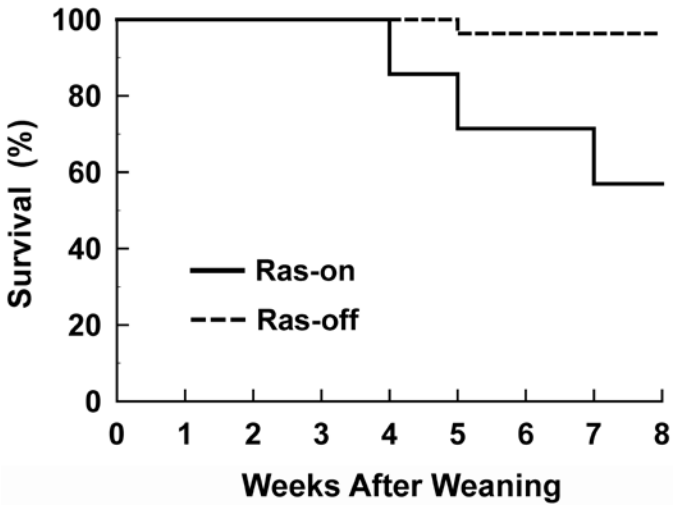

Figure 3. Survival of M/R mice with continuous Ras activation (Ras-on, solid line, 8 wk, $n = 21$) or with 4 wk Ras activation (solid line) followed by an additional 4 wk subsequent to discontinuation of Ras (dashed line, $n = 27$). Ras activation was begun at weaning (week 0). Mice were removed from study once they developed advanced heart failure or at study end (week 8).

wk of Ras activation, 15 of 21 (71.5%) hearts had hypertrophic lesions, and the majority of these lesions were mild (14 of 15 mice had lesion scores of 1; Figure 4 A). Lesion severity increased with 2 additional weeks of Ras activation; 4 wk of Ras activation induced cardiomyopathy in 22 of 28 (78.6%) hearts, the majority of which (15 of 22) were lesion score of 3 (most severe; Figure 4 B).

Cardiomyopathy in mice with 2 or 4 weeks of Ras activation was subsequently compared with that in mice that had Ras activation discontinued for 1 or 4 weeks after initial induction, to determine whether Ras-induced cardiomyopathy could resolve (Figure 1 A). Disease severity worsened or remained similar 1 wk after Ras activity was halted (Figure 4 A and B). At 4 wk after discontinuation of Ras activity, the incidence and severity of cardiac lesions were less than those observed at 1 wk after discontinuation of Ras-12V (Figure 4 A and B), suggesting partial resolution of pathogenic myocardial hypertrophy after the peak of disease severity. No cardiac lesions were observed in any littermate control (wild type, M, and R) or genotype-matched control (M/R mice without Ras activation) mice.

Ras manipulation influenced HW:BW ratios. HW:BW ratios for M/R mice with 4 wk of Ras activation were significantly ($P < 0.01$) increased compared with those of age-matched control mice (Figure 4 C). Increased HW:BW ratio was also present 1 wk after Ras was discontinued, coinciding with histologic evidence of myocardial lesion progression as determined by lesion scores. However, HW:BW ratios did not differ ($P = 0.21$) between M/R and treatment- and age-matched control mice at 4 wk after discontinuing Ras-12V expression. When M/R mice with 4 wk of Ras-on were compared with other groups, HW:BW ratios of mice allowed 4 wk of recovery were significantly ($P < 0.03$) lower than those of the mice with 0- or 1-wk recovery periods (Figure 4 C). The HW:BW kinetic pattern was in general agreement with lesion score analysis, strongly implicating the presence of recovery mechanisms that allowed hearts to repair (at least in part) Ras-induced hypertrophic myocardial injury at 4 wk after Ras activity was turned off. In addition, M/R mice with 2 wk of Ras activation showed significantly ($P = 0.01$) lower HW:BW ratios after 4 wk of recovery time than did mice with 1 wk of recovery only (data not shown). Influence on HW:BW ratio was attributed to changes in HW that were induced by Ras activation in M/R hearts, given that no differences in BW between M/R mice and control mice were noted at 2 wk ($P = 0.36$), 4 wk ($P = 0.20$), and 8 wk ($P = 0.52$; data not shown). Although the potential for differences in HW:BW between male and female mice was considered, sex-associated effects on HW:BW ratios were not significant ($P > 0.35$).

Levels of Ras, pERK1/2, ANF, and cell-cycle regulators were altered during the induction and resolution of pathogenic myocardial hypertrophy. Evidence of elevated Ras levels and activation (phosphorylation) of the downstream effector ERK1/2 was investigated in M/R mice by using immunohistochemistry and immunofluorescence. Intense Ras immunolabeling was localized to hypertrophic cardiomyocytes, whereas less-affected myocytes had minimal or no labeling (Figure 5 A). On serial tissue sections, pERK1/2 immunolabeling correlated with the areas of positive Ras labeling (Figure 5 B). The extent and intensity of immunolabeling was more pronounced in hearts with 4 wk compared with 2 wk of Ras-12V expression, correlating with the lesion scores in those hearts. To further demonstrate that activation of Ras signaling occurred in cardiomyocytes expressing Ras-12V, Ras and pERK double-immunolabeling was carried out (Figure 5 D through F). Colocalization of both Ras and pERK1/2 in hypertrophic cardiomyocytes demonstrated a direct correlation for induced Ras-12V expression with ERK1/2 activation and disease phenotype. Overall, the immunohistology revealed increased Ras–MAPK signaling in hypertrophic cardiomyocytes. In addition, Ras levels and activation status of pERK were analyzed in hearts allowed recovery time by turning off Ras-12V expression after Ras activation. By 4 wk of Ras-off, Ras had decreased to basal levels (Figure 5 G), whereas residual pERK1/2 remained in small focal areas of morphologically normal cardiac myocytes (Figure 5 H).

Protein levels of Ras and MAPK during induction and resolution of pathogenic myocardial hypertrophy were examined further by using Western blot analysis. Due to the variation in cardiac lesion scores within the same experimental group, multiple heart specimens were examined, and representative results are shown (Figure 6). Robust Ras levels were detected in hearts with 2 and 4 wk of Ras activation. The quantity of Ras protein decreased notably after discontinuing Ras-12V expression for 1 wk, despite progression of pathogenic myocardial hypertrophy. Therefore, attenuation of Ras protein preceded the improvement in cardiomyopathy, as evidenced by both histopathology and HW:BW ratio. By 4 wk after discontinuing Ras-12V expression, Ras protein was no longer detectable, as in control mice (Figure 6).

Activation of ERK1/2 was evident at 2 wk after Ras activation in M/R hearts and subsided once Ras-12V expression had been discontinued for 1 wk. By contrast, in mice that had 4 wk of Ras activation, ERK1/2 activation persisted 1 wk after Ras-12V expression was discontinued whereas Ras-12V protein levels were greatly diminished (Figure 6). In both cohorts, 4 wk after discontinuing the stimulus for Ras, ERK1/2 activity was reduced to basal levels, in agreement with immunohistochemistry results. In addition to activation, ERK1/2 protein levels were higher in mice with 4 wk than with 2 wk of Ras activation. Interestingly, in addition to the elevated ERK1/2 activity from 2 wk to 4 wk of Ras activation, a shift in the subcellular distribution pattern of pERK

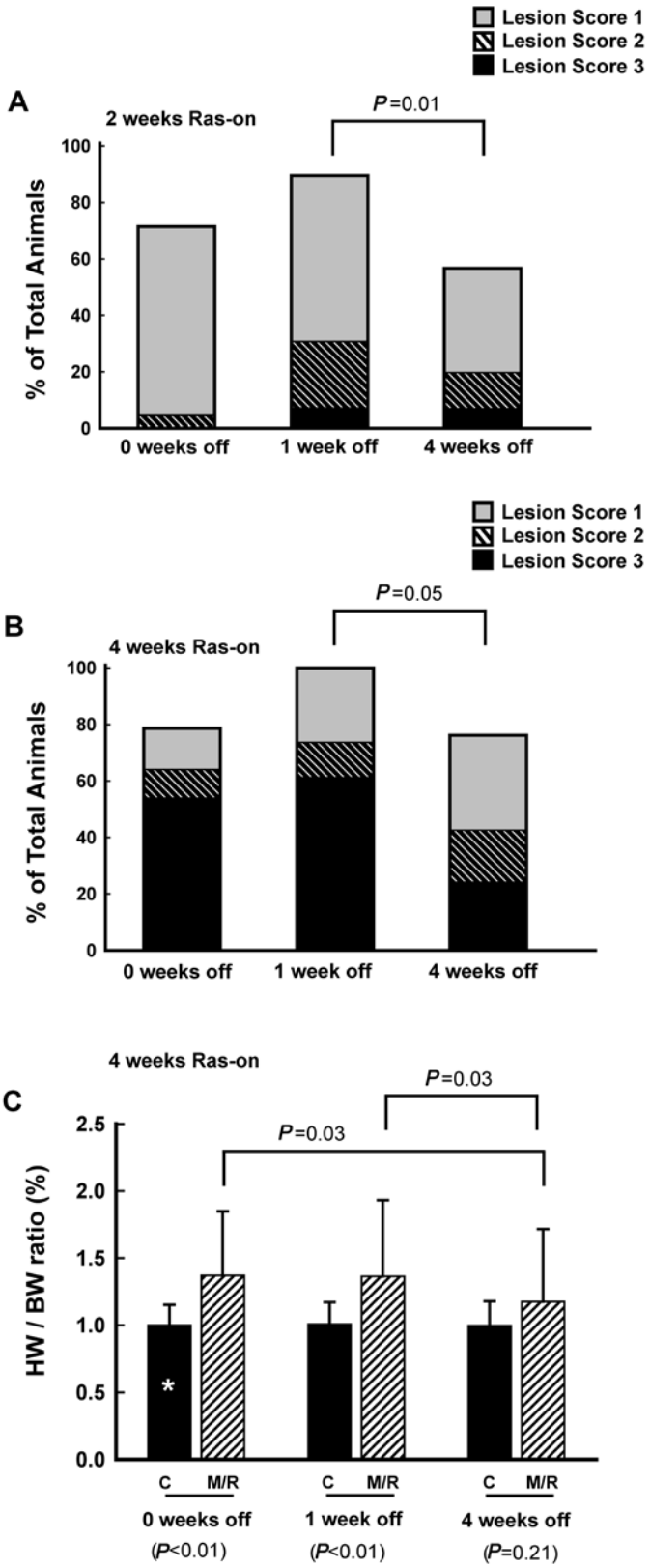

Figure 4. Extent of pathogenic myocardial hypertrophy development in M/R mice during and after Ras activation. Percentage of mice exhibiting cardiac lesion scores of 1 through 3 with (A) 2 wk or (B) 4 wk of Ras activation (Ras-on). Each bar represents mice given different periods during which Ras activation was discontinued for 0, 1, or 4 wk (Ras-off). Lesion scores (described in Table 1) of 1 (light gray), 2 (hatched), and 3 (black) are indicated for mice in each group. Significant difference was shown between the groups with Ras discontinuation for 1 wk (peak disease severity) and 4 wk. C) Heart weight (HW) to body weight (BW) ratios for M/R mice with 4 wk of Ras activation, followed by 0, 1, or 4 wk of Ras-off (hatched bars), as compared with matched control mice (solid bars). All HW:BW data are expressed relative to those of the 4-wk control mice (4 wk Ras-on, 0 wk Ras-off group [*]) set at a value of 1.0 (that is, the norm-referenced HW:BW ratio). Each group of control mice was matched individually for age and time on study for each respective M/R treatment group. Numbers of mice in groups are shown in Figure 1. Statistical analysis was performed between M/R mice and matched controls as well as between M/R groups; *P* values are indicated.

within cardiomyocytes occurred as disease progressed. pERK was predominantly intranuclear with 2 wk of Ras activation but was distributed more frequently in the cytoplasm at 4 wk of Ras activation (inset of Figure 5 B). The activation of Ras–ERK1/2 signaling was accompanied by the induction of ANF (a hallmark protein reexpressed by adult cardiomyocytes in response to cardiac hypertrophy and congestive heart failure) in M/R hearts from mice with either 2 or 4 wk of Ras activation (Figure 6). No significant changes in activation or expression of p38 or c-Jun-NH_2-terminal kinase were detected by using Western blotting (data not shown), in agreement with another cardiac Ras-12V transgenic model.[20]

In the present study, Ras–ERK1/2 signaling implicated the potential for cell-cycle reactivation in cardiomyocytes. Classically, cardiomyocytes withdraw from the cell cycle postnatally, and the fate of cell-cycle reentry in response to injuries is poorly understood. We used Western blotting to determine whether cell-cycle–related protein production was altered in cardiomyocytes during progression and resolution of Ras-induced cardiomyopathy. With 2 wk of Ras activation, levels of cyclins B1 and D1 were increased in some mice (Figure 6). By 1 wk after discontinuation of Ras activation and thereafter, levels of cyclins B1 and D1 approximated basal levels. However, the M/R mice with 4 wk of Ras activation showed greater increases in cyclin B1 and D1 levels compared with those of mice with 2 wk of Ras activation, and the robust expression persisted 1 wk after discontinuing Ras-12V transgene stimulation. By 4 wk without Ras activity (after 4 wk of Ras activation), cyclin B1 was diminished, although it remained above basal levels in some M/R mice; however, levels of cyclin D1 were similar to those in control hearts (Figure 6). In general, the pattern of cyclin levels was commensurate with disease severity. As an important regulator for G_2/M cell-cycle transition, the cyclin B–cdc2 complex facilitates completion of the cell cycle. Western blotting revealed increased phosphorylation of cdc2 at Tyr15, an inactive form of cdc2, in hearts with 4 wk of Ras activation, implying a functional block to cell-cycle progression through M phase at this stage (Figure 6). The levels of cyclins A and E in M/R mice were similar to those in control mice (data not shown); therefore these factors did not appear to contribute to cell-cycle regulation during pathogenic myocardial hypertrophy induction and recovery in the same manner as did cyclins B1 and D1.

The kinetics of cardiac PCNA production paralleled those of cyclins B1 and D1. Elevated PCNA production was observed in hearts after 2 wk of Ras activation, and PCNA returned to basal levels when Ras activation was discontinued (Figure 6). More ro-

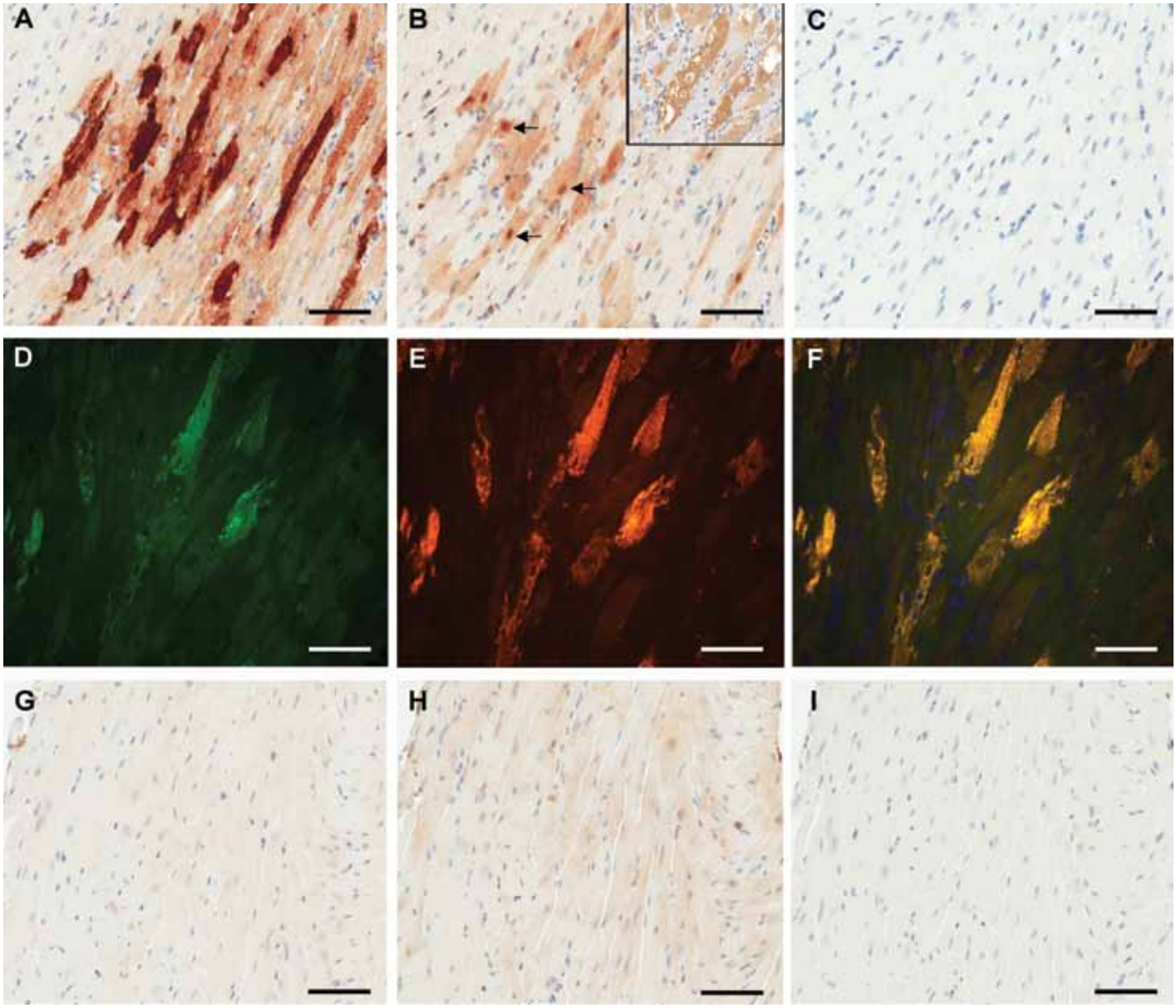

Figure 5. Ras and pERK1/2 levels in M/R hearts. Representative immunohistochemistry labeling of (A) Ras and (B) pERK1/2 in serial sections of myocardium from an M/R mouse with 2 wk of Ras activation. In M/R hearts with 2-wk Ras activation, immunohistochemistry revealed both nuclear and cytoplasmic localization of pERK1/2 (arrows). Mostly cytoplasmic accumulation of pERK1/2 was observed after 4 wk of Ras activation (inset photomicrograph). (C) Ras immunohistochemistry on an M/R control heart lacking Ras-12V transgene induction revealed minimal labeling. Double immunofluorescent labeling of (D) Ras and (E) pERK1/2 was used to further demonstrate representative colocalization of Ras and pERK1/2 within a hypertrophic M/R heart with 4 wk of Ras activation. F) Optically merged photomicrograph to document coexpression of Ras and pERK1/2 in the same hypertrophic cardiomyocytes (yellow). (G through I) Representative (G) Ras and (H) pERK1/2 expression in serial sections from an M/R heart with 4 wk Ras-on and subsequent 4 wk Ras-off. Minimal Ras production and residual pERK occur in myocardium lacking hypertrophic myocytes. (I) A negative control lacking primary antibody. Overall, Ras and pERK1/2 immunohistochemical assays were performed on 49 mice, including 35 M/R mice, and were distributed among the various treatment groups. Bar, 50 µm.

bust PCNA expression was observed in mice with 4 wk of Ras-on; the level of PCNA was concomitant with lesion score, persisted 1 wk after Ras was discontinued, and declined by 4 wk after Ras was discontinued.

Expression of the Cip/Kip family of cyclin-dependent kinase inhibitors (p21, p27, and p57) was examined because of their broad inhibitory roles at various points of the cell cycle.[16,17] With 2 wk of Ras activation, protein levels of cyclin-dependent kinase inhibitors increased compared with the baseline expression level (Figure 6). The expression of all 3 cyclin-dependent kinase inhibitors returned to this basal level after discontinuing Ras activity for 1 wk. Mice with 4 wk of Ras activation showed increased levels of all 3 cyclin-dependent kinase inhibitors. p21 and p27 production were decreased from these levels 1 wk after the Ras-12V transgene was turned off and were similar to or at the basal levels by 4 wk. The p57 response differed in that its greatest expression level

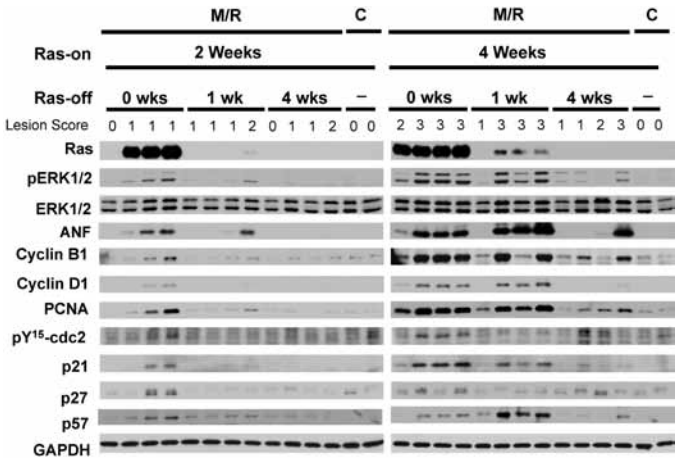

Figure 6. Western blot analysis of Ras, pERK1/2, ANF, and cell-cycle regulators in individual hearts of M/R and control (C) mice. Samples during and after induction of Ras-12V expression are included. Representative results are shown for mice with 2 and 4 wk of Ras activation (Ras-on), as well as for mice that had Ras discontinued for either 0, 1, or 4 wk after initial induction (Ras-off). Lesion score of each heart (as defined in Figure 2) is indicated. Analyses are shown for Ras, pERK1/2, total ERK1/2, ANF, and cell-cycle associated proteins, PCNA, cyclin B1, cyclin D1, pY^{15}-cdc2, and the cyclin-dependent kinase inhibitors p21, p27, and p57.

was observed at 1 wk after Ras was discontinued (Figure 6). Peak p57 expression coincided with the increased production of cyclins B1 and D1—at the same time that myocardial lesions were most severe (Figure 4).

Phosphohistone H3 and Aurora B kinase immunohistochemistry were performed to determine whether Ras signaling was sufficient to carry cardiomyocytes through cell cycle to complete mitosis and cytokinesis, respectively. The lack of phosphohistone H3 and Aurora B kinase immunohistochemistry labeling in cardiomyocytes, as well as the absence of mitotic nuclear morphology, indicated that cell replication did not occur in hypertrophic cardiomyocytes (data not shown).

Discussion

Ras signal transduction influences cytoproliferation, differentiation, and cell survival in a variety of cell types.[21,27] In the heart, activation of Ras predominantly led to myocardial hypertrophy.[15] In M/R transgenic mice, Ras activation promoted downstream ERK1/2 MAPK activation, initiated ANF expression, and induced pathogenic cardiomyocyte hypertrophy that progressed to maladaptive congestive heart failure. The longer-term effects of Ras activation in these M/R mice are similar to several of the cardiac lesions caused by Ras in other mouse models.[11,41] Moreover, the current M/R model recapitulates human cardiomyocyte hypertrophy similar to that seen secondary to a variety of physiologic agonists capable of activating endogenous Ras signaling events.[8,30] The findings of chronic disease progression in our model provide clear evidence of the similarity to late-stage cardiomyopathy in human heart disease; however, the main study design focus was to investigate early pathogenic cardiomyocyte hypertrophy and its potential for resolution.

The inducible cardiac activation of Ras in M/R mice was controlled by using a tet-off system that acted through the heart-specific α-myosin heavy chain promoter,[40] providing 2 key advantages over other animal models of heart-specific Ras activation. Ras-12V gene expression and subsequent protein production was initiated when cardiomyocytes became mature in weaned mice. This capability minimized the potentially confounding influence introduced by abnormal Ras activity during embryogenesis and early postnatal development, when active cardiomyocyte proliferation is ongoing.[1] Furthermore, the tet-off system allowed subsequent discontinuation of Ras activation after the initial hypertrophic myocardial disease induction in M/R mice, permitting observation of recovery from injury. Expression of the Ras-12V transgene and activation of signals downstream of Ras were conspicuously altered in M/R hearts with such regulation. Collective evidence for myocardial lesion resolution after cessation of Ras activation included reduced HW:BW ratio, improved pathologic lesion scores, and improved survival. Cardiomyopathy initially persisted or worsened 1 wk after discontinuation of Ras-12V expression, despite greatly diminished Ras levels. This transiently sustained hypertrophy likely was associated with residual downstream activities of effectors, including ERK1/2, as demonstrated in our mice that had 4 wk of Ras activation. The current study is the first to document the reversible nature of myocardial injury induced by Ras activation that has the capacity to progress to pathogenic myocardial hypertrophy and congestive heart failure.

Cell-cycle regulatory proteins increasingly are thought to play a key role in cardiac hypertrophy.[1,3] Signs of cell-cycle reentry, such as elevated expression of G_1 cyclin–cyclin dependent kinase[18,24,42] and coincident downregulation of cyclin-dependent kinase inhibitors,[16] have been reported in hypertrophic cardiomyocytes. Reciprocally, inhibition of G_1 cyclin–cyclin dependent kinase activity in mature cardiomyocytes blocks such hypertrophy.[22,32] Activation of Ras signaling in M/R mice led to indications of cell-cycle reentry. In particular, elevated expression of PCNA and cyclins D1 and B1 was associated with morphologic evidence of increased DNA (karyomegaly) and protein synthesis (increased cell size). Resolution of myocardial hypertrophy in this model was accompanied by evidence that cells were capable of executing a coordinated exit from the reactivated cell cycle. Diminished expression of PCNA and cyclins B1 and D1, as well as cyclin-dependent kinase inhibitors and other cycle inhibitory factors, coincident with the reversibility of myocardial hypertrophy in M/R mice provides

additional evidence of the mechanistic association between cardiomyocyte hypertrophy and cell-cycle regulation.

Adult cardiomyocytes are capable of proliferating when the appropriate signals are provided.[26,36] However, completion of cell division was not evident when Ras alone was activated in M/R mice. In the current study, upregulation of cyclin production was not accompanied by increased numbers of mitotic figures or expression of mitotic markers such as histone H3 phosphorylation (mitosis) and increased Aurora B kinase (cytokinesis). In contrast to the situation for cyclins B1 and D1, no significant increase in cyclin A levels was detected in M/R hearts. Overexpression of cyclin A in vivo promotes cell-cycle reentry and myocardial regeneration in ischemic hearts.[39] In addition, cyclin A–cyclin dependent kinase complexes are central to transition from S to G_2 phases, wherein cyclin B–cdc2 activity becomes crucial for driving mitosis.[10] In hypertrophic M/R hearts, basal levels of cyclin A expression coupled with an increase in the inactive form of cdc2 (pTyr15) may have contributed to an inability of cyclinB–cdc2 to catalyze progression to G_2 and M phases, despite elevated cyclin B expression.

In addition, the increase in pTyr15–cdc2 and lack of cyclin A upregulation were accompanied by unanticipated increases in cell-cycle inhibitor levels in M/R hearts. Expression of cyclin-dependent kinase inhibitors increases in cardiomyocytes after birth, in association with cell-cycle exit and differentiation.[4,17] Consistent with this, proliferating cardiomoycytes downregulate their expression of p21 and p27 cyclin-dependent kinase inhibitors in response to cyclin D overexpression.[6] In contrast, increased expression of p21, p27, or p57 (cyclin-dependent kinase inhibitors) was observed in 3 of 4 M/R mice. This response appeared to be influenced by the duration of Ras activation and the extent of hypertrophy. We interpreted these reciprocal increases in cyclin-dependent kinase inhibitors, appearing concurrently with increased cyclin expression, additional checks to the unconventional cell cycle reentry induced by activation of Ras signaling. Overall, signaling events after Ras activation were insufficient to stimulate proliferation of mature cardiomyocytes in vivo.

Activation of ERK MAPK in hypertrophic cardiomyocytes from M/R hearts by 2 wk of Ras activation was further increased at 4 wk. ERK was the predominant MAPK activated by Ras signaling in M/R hearts. The kinetics of ERK activation coincided with elevations of Ras and cyclins B1and D1 during the course of this study. This result is in agreement with ERK1/2 functioning as a cell-cycle activator.[7] In addition, the subcellular localization of pERK is an important factor contributing to ERK function and the fate of cells. Nuclear localization of pERK is essential for cell-cycle progression, whereas cytosolic accumulation of pERK induces proapoptotic responses.[5,19] The subcellular localization of pERK in M/R cardiomyocytes appeared to correlate with disease severity. With prolonged Ras activation (4 and 8 wk), pERK was retained more often within the cytosol of hypertrophic M/R cardiomyocytes, and intranuclear localization was reduced compared with the predominant intranuclear targeting of pERK seen at 2 wk of Ras activation. A plausible hypothesis is that the limited nuclear localization of pERK, observed during late-stage cardiomyopathy, contributed to the incomplete cell cycle. Furthermore, retention of pERK in the cytosol may have triggered programmed cell death, resulting in the cell loss observed at later stages of myocardial hypertrophy in M/R hearts (characterized by morphologic evidence of cell death, caspase 3 activation, cardiomyocyte loss, and fibrosis in hearts after 8 wk of Ras-12V induction). Nevertheless, the reversible nature of the pathogenic myocardial hypertrophy after as long as 4 wk of Ras activation indicated that programmed cell death is unlikely to be a committed fate during early induction of hypertrophy.

Reintroduction of doxycycline-containing mouse ration provided the experimental conditions for cardiac hypertrophy resolution. Cognizance of a potential healing benefit due to administration of the agent used for controlling Ras activation is important. Previously, supplying 6 mg/mL doxycycline in drinking water was demonstrated to alleviate isoproterenol- or aortic banding-induced cardiac hypertrophy.[9] In the published model, a doxycycline dose in the range of 18 mg daily was necessary to ensure statistically significant reductions in cardiac hypertrophy. In addition, the human allometric doxycycline dose was ineffective in reducing heart mass in this model.[9] In contrast to improvement in cardiac hypertrophy as a consequence of doxycycline, a concurrently published study documented complications resulting in hypertrophy augmentation with 5 mg doxycycline daily.[37] We considered potential confounding effects of doxycycline administration on recovery from cardiac hypertrophy in *ras* transgenic mice. Moreover, the estimated dose of doxycycline in mice on the present study (0.8 mg daily) is less than 5% of the daily intake required for regression of hypertrophy by doxycycline.[9] The doxycycline dose, supplied during Ras-off recovery phases in the present study, more closely mimicked the human allometric doxycycline dose, and therefore was considered unlikely to provide any therapeutic benefit for hypertrophic cardiac myocytes in Ras-12V transgenic mice.

The current M/R model enables the manipulation of Ras activation, providing unique opportunities to study molecular mechanisms governing an important signaling pathway involved in cardiac hypertrophy and cardiomyopathy. Alterations in cell-cycle factors were directly associated with the timing for induction and resolution of pathogenic myocardial hypertrophy in the model. After eventual resolution of cardiomyopathy, most protein inducers and inhibitors of the cell cycle that we studied approximated basal levels similar to those in control mice, consistent with exit from the reactivated cell cycle. Our findings support a premise that a balance between cell-cycle activators and inhibitors may help to determine whether cardiomyocytes undergo hypertrophic or hyperplastic growth after mitogenic stimulation.[2] Strategies can be designed for targeting cardiomyocyte cell-cycle regulatory activities to assess whether the approach can facilitate recovery or repair of hypertrophic lesions.

Acknowledgments

The study was supported by the Intramural Research Program, Center for Cancer Research, National Cancer Institute, Bethesda, Maryland. We acknowledge the scholarly support provided by Jennifer Edwards and Joshua Webster. All authors declare there are no actual or potential conflicts of interest, including any financial, personal, or other relationships with people or organizations that could inappropriately influence this work.

Bih-Rong Wei and Philip L Martin are employees of the Science Applications International Corporation–Frederick, Frederick, Maryland, on contract to the National Cancer Institute Intramural Research Program (Award N01-CO-12400).

References

1. **Ahujas P, Sdek P, MacLellan WR.** 2007. Cardiac myocyte cell-cycle control in development, disease, and regeneration. Physiol Rev **87:**521–544.
2. **Bicknell KA, Brooks G.** 2008. Reprogramming the cell-cycle machinery to treat cardiovascular disease. Curr Opin Pharmacol **8:**193–201.

3. **Bicknell KA, Surry EL, Brooks G.** 2003. Targeting the cell-cycle machinery for the treatment of cardiovascular disease. J Pharm Pharmacol **55:**571–591.
4. **Brooks G, Poolman RA, Li JM.** 1998. Arresting developments in the cardiac myocyte cell cycle: role of cyclin-dependent kinase inhibitors. Cardiovasc Res **39:**301–311.
5. **Brunet A, Roux D, Lenormand P, Dowd S, Keyse S, Pouyssegur J.** 1999. Nuclear translocation of p42/p44 mitogen-activated protein kinase is required for growth-factor–induced gene expression and cell-cycle entry. EMBO J **18:**664–674.
6. **Busk PK, Hinrichsen R, Bartkova J, Hansen AH, Christoffersen TE, Bartek J, Haunso S.** 2005. Cyclin D2 induces proliferation of cardiac myocytes and represses hypertrophy. Exp Cell Res **304:**149–161.
7. **Chambard JC, Lefloch R, Pouyssegur J, Lenormand P.** 2007. ERK implication in cell-cycle regulation. Biochim Biophys Acta **1773:**1299–1310.
8. **Clerk A, Cullingford TE, Fuller SJ, Giraldo A, Markou T, Pikkarainen S, Sugden PH.** 2007. Signaling pathways mediating cardiac myocyte gene expression in physiological and stress responses. J Cell Physiol **212:**311–322.
9. **Errami M, Galindo CL, Tassa AT, Dimaio JM, Hill JA, Garner HR.** 2008. Doxycycline attenuates isoproterenol- and transverse aortic banding-induced cardiac hypertrophy in mice. J Pharmacol Exp Ther **324:**1196–1203.
10. **Fung TK, Ma HT, Poon RY.** 2007. Specialized roles of the 2 mitotic cyclins in somatic cells: cyclin A as an activator of M phase-promoting factor. Mol Biol Cell **18:**1861–1873.
11. **Hunter JJ, Tanaka N, Rockman HA, Ross J Jr, Chien KR.** 1995. Ventricular expression of a MLC-2v-ras fusion gene induces cardiac hypertrophy and selective diastolic dysfunction in transgenic mice. J Biol Chem **270:**23173–23178.
12. **Institute for Laboratory Animal Research.** 1996. Guide for the care and use of laboratory animals. Washington (DC): National Academies Press.
13. **Kai H, Muraishi A, Sugiu Y, Nishi H, Seki Y, Kuwahara F, Kimura A, Kato H, Imaizumi T.** 1998. Expression of protooncogenes and gene mutation of sarcomeric proteins in patients with hypertrophic cardiomyopathy. Circ Res **83:**594–601.
14. **Komuro I, Kurabayashi M, Takaku F, Yazaki Y.** 1988. Expression of cellular oncogenes in the myocardium during the developmental stage and pressure-overloaded hypertrophy of the rat heart. Circ Res **62:**1075–1079.
15. **Lezoualc'h F, Metrich M, Hmitou I, Duquesnes N, Morel E.** 2008. Small GTP-binding proteins and their regulators in cardiac hypertrophy. J Mol Cell Cardiol **44:**623–632.
16. **Li JM, Brooks G.** 1997. Downregulation of cyclin-dependent kinase inhibitors p21 and p27 in pressure-overload hypertrophy. Am J Physiol **273:**H1358–H1367.
17. **Li JM, Brooks G.** 1999. Cell-cycle regulatory molecules (cyclins, cyclin-dependent kinases, and cyclin-dependent kinase inhibitors) and the cardiovascular system: potential targets for therapy? Eur Heart J **20:**406–420.
18. **Li JM, Poolman RA, Brooks G.** 1998. Role of G1 phase cyclins and cyclin-dependent kinases during cardiomyocyte hypertrophic growth in rats. Am J Physiol **275:**H814–H822.
19. **Mebratu Y, Tesfaigzi Y.** 2009. How ERK1/2 activation controls cell proliferation and cell death: is subcellular localization the answer? Cell Cycle **8:**1168–1175.
20. **Mitchell S, Ota A, Foster W, Zhang B, Fang Z, Patel S, Nelson SF, Horvath S, Wang Y.** 2006. Distinct gene expression profiles in adult mouse heart following targeted MAP kinase activation. Physiol Genomics **25:**50–59.
21. **Molina JR, Adjei AA.** 2006. The Ras–Raf–MAPK pathway. J Thorac Oncol **1:**7–9.
22. **Nozato T, Ito H, Watanabe M, Ono Y, Adachi S, Tanaka H, Hiroe M, Sunamori M, Marum F.** 2001. Overexpression of Cdk inhibitor p16INK4a by adenovirus vector inhibits cardiac hypertrophy in vitro and in vivo: a novel strategy for the gene therapy of cardiac hypertrophy. J Mol Cell Cardiol **33:**1493–1504.
23. **Oh WJ, Rishi V, Pelech S, Vinson C.** 2007. Histological and proteomic analysis of reversible H-RasV12G expression in transgenic mouse skin. Carcinogenesis **28:**2244–2252.
24. **Poolman RA, Brooks G.** 1998. Expressions and activities of cell-cycle regulatory molecules during the transition from myocyte hyperplasia to hypertrophy. J Mol Cell Cardiol **30:**2121–2135.
25. **Proud CG.** 2004. Ras, PI3 kinase, and mTOR signaling in cardiac hypertrophy. Cardiovasc Res **63:**403–413.
26. **Regula KM, Rzeszutek MJ, Baetz D, Seneviratne C, Kirshenbaum LA.** 2004. Therapeutic opportunities for cell cycle re-entry and cardiac regeneration. Cardiovasc Res **64:**395–401.
27. **Roberts PJ, Der CJ.** 2007. Targeting the Raf–MEK–ERK mitogen-activated protein kinase cascade for the treatment of cancer. Oncogene **26:**3291–3310.
28. **Ruan H, Mitchell S, Vainoriene M, Lou Q, Xie LH, Ren S, Goldhaber JI, Wang Y.** 2007. G_i α1-mediated cardiac electrophysiological remodeling and arrhythmia in hypertrophic cardiomyopathy. Circulation **116:**596–605.
29. **Stansfield WE, Rojas M, Corn D, Willis M, Patterson C, Smyth SS, Selzman CH.** 2007. Characterization of a model to independently study regression of ventricular hypertrophy. J Surg Res **142:**387–393.
30. **Sugden PH.** 2001. Signalling pathways in cardiac myocyte hypertrophy. Ann Med **33:**611–622.
31. **Sugden PH.** 2003. Ras, Akt, and mechanotransduction in the cardiac myocyte. Circ Res **93:**1179–1192.
32. **Sugden PH, Clerk A.** 1998. Cellular mechanisms of cardiac hypertrophy. J Mol Med **76:**725–746.
33. **Sugden PH, Clerk A.** 2000. Activation of the small GTP-binding protein Ras in the heart by hypertrophic agonists. Trends Cardiovasc Med **10:**1–8.
34. **Tamamori M, Ito H, Hiroe M, Terada Y, Marumo F, Ikeda MA.** 1998. Essential roles for G1 cyclin-dependent kinase activity in development of cardiomyocyte hypertrophy. Am J Physiol **275:**H2036–H2040.
35. **Thorburn A, Thorburn J, Chen SY, Powers S, Shubeita HE, Feramisco JR, Chien KR.** 1993. hRas-dependent pathways can activate morphological and genetic markers of cardiac muscle cell hypertrophy. J Biol Chem **268:**2244–2249.
36. **van Amerongen MJ, Engel FB.** 2008. Features of cardiomyocyte proliferation and its potential for cardiac regeneration. J Cell Mol Med **12:**2233–2244.
37. **Vinet L, Rouet-Benzineb P, Marniquet X, Pellegrin N, Mangin L, Louedec L, Samuel JL, Mercadier JJ.** 2008. Chronic doxycycline exposure accelerates left ventricular hypertrophy and progression to heart failure in mice after thoracic aorta constriction. Am J Physiol Heart Circ Physiol **295:**H352–H360.
38. **Wei BR, Hoover SB, Ross MM, Zhou W, Meani F, Edwards JB, Spehalski EI, Risinger JI, Alvord WG, Quinones OA, Belluco C, Martella L, Campagnutta E, Ravaggi A, Dai RM, Goldsmith PK, Woolard KD, Pecorelli S, Liotta LA, Petricoin EF, Simpson RM.** 2009. Serum S100A6 concentration predicts peritoneal tumor burden in mice with epithelial ovarian cancer and is associated with advanced stage in patients. PLoS ONE **4:**e7670.
39. **Woo YJ, Panlilio CM, Cheng RK, Liao GP, Atluri P, Hsu VM, Cohen JE, Chaudhry HW.** 2006. Therapeutic delivery of cyclin A2 induces myocardial regeneration and enhances cardiac function in ischemic heart failure. Circulation **114:**I206–I213.
40. **Yu Z, Redfern CS, Fishman GI.** 1996. Conditional transgene expression in the heart. Circ Res **79:**691–697.
41. **Zheng M, Dilly K, Dos Santos Cruz J, Li M, Gu Y, Ursitti JA, Chen J, Ross J Jr, Chien KR, Lederer JW, Wang Y.** 2004. Sarcoplasmic reticulum calcium defect in Ras-induced hypertrophic cardiomyopathy heart. Am J Physiol Heart Circ Physiol **286:**H424–H433.
42. **Zhong W, Mao S, Tobis S, Angelis E, Jordan MC, Roos KP, Fishbein MC, de Alboran IM, MacLellan WR.** 2006. Hypertrophic growth in cardiac myocytes is mediated by Myc through a cyclin D2-dependent pathway. EMBO J **25:**3869–3879.